13th ewtec 2019 Proceedings of the 13th European Wave and Tidal Energy Conference 1-6 Sept 2019, Naples, Italy

Sensitivity of bathymetry and choice of tidal constituents on tidal-stream energy resource characterization in the Gulf of California, Mexico

Carlos J. Mejia-Olivares, Ivan D. Haigh, Matt J. Lewis and Simon P. Neill

Abstract— **Resource assessments are essential, yet many are based on hydrodynamic models forced with coarse global data products for bathymetry and open-boundary forcing. The aim of this paper is to examine how selection of: (1) two open source bathymetry products (GEBCO and ETOPO) and the inclusion of a higher-resolution bathymetry survey; and (2) considering different numbers of tidal constituents; affects the quantification of the tidal-stream energy resource for the Gulf of California. For the location with fastest current speeds, a 18 km wide passage between the San Lorenzo and San Esteban Islands, (herein San Lorenzo Passage), the annual mean power was estimated at around 120 MW and 20 MW when using freely available bathymetry data (GEBCO and ETOPO respectively), but increased to ~200 MW when using a bespoke dataset that was a combination of GEBCO and higher resolution bathymetry. Integrating higher resolution of bathymetry data within the model simulations increase the accuracy to resolve flows within the midriff region. We also compared the estimated energy computed using 29 tidal constituents compared with simulations that included just the M_2 and S_2 tidal constituents. The annual mean kinetic power density decreased by almost 1/3rd in the channel between San Lorenzo and San Esteban Islands, when considering just the M_2 and S_2 constituents, suggesting that diurnal and higher order harmonic constituents are important for accurate resource assessments in this region.**

Keywords— **Annual mean power, bathymetry, Gulf of California, México, sensitivity test, tidal-stream energy.**

I. Introduction

OVER the last two decades there has been increased interest in tidal energy exploitation [1]. Tidal energy offers many benefits compared to other sources of renewable energy, because of the regular and predictable nature of tides [2]. This paper focusses on tidal-stream energy; the generation of electricity by harvesting the kinetic energy of moving water to power turbines. These type of devices use similar concepts to wind turbines. The main differences are the increased flow density and the thrust that each device is capable of tolerating in regular operational conditions.

Many past studies have undertaken tidal-stream energy resource assessments for different regions around the world using a variety of modelling techniques and methodologies, e.g., [3]-[9]. In these studies, a variety of different bathymetry products, boat surveys and/or bathymetry charts are used, e.g. [10]-[15] in their hydrodynamic model simulations for tidal-stream energy assessments, and different combinations of tidal constituents are used to force boundary conditions. It is pertinent, therefore, to consider how different bathymetry products and varying combinations of tidal constituents affects the quantification of the tidal-stream energy resource.

The overall aim of this paper is to examine how choice of bathymetry product and tidal constituents affects the quantification of the tidal-stream energy resource. As a case study we consider the Gulf of California (hereafter GC), building on the previous study of [16], who undertook the first tidal-stream energy resource assessment in the Gulf of California. We undertake sensitivity tests in which we estimate and compare the maximum theoretical undisturbed mean KPD (Kinetic

Paper ID number: 1214; Conference track: Tidal resource characterization. This research was financed by two sponsorships: CONACyT (the National Council of Science and Technology) through the grant "Becas en el extranjero 2014-1" grant reference CVU 536867 and by the University of Southampton.

C. J. Meja-Olivares and I. D. Haigh are with Ocean and Earth Science, National Oceanography Centre, University of Southampton, European Way, Southampton, SO14 3ZH, U.K. (e-mail: carlos.mejia-olivares@noc.soton.ac.uk, I.D.Haigh@soton.ac.uk).

M. J. Lewis and S.P. Neill are with School of Ocean Sciences, Bangor University, U.K (email: m.j.lewis@bangor.ac.uk, s.p.neill@bangor.ac.uk).

Power Density) and annual mean power output calculated from hydrodynamic model runs that use: (1) just GEBCO bathymetry data [17], (2) just the ETOPO bathymetry [18] and (3) GEBCO data merged with higher resolution data from CICESE (The Centre for Scientific Research and Higher Education at Ensenada), for the upper part of the Gulf of California. We also examine how the choice of different tidal constituents affects the quantification of a tidal-stream energy resource for the Gulf of California, particularly since the region is characterized by mixed diurnal and semidiurnal tides.

The structure of the paper is as follows: The model configuration and validation is described in Section II. Sensitivity methods are describe in section III. We discuss the results of the sensitivity test in Section IV. Finally, conclusion are given in Section V.

II. METHODS

A. *Gulf of California model configuration and validation*

The Gulf of California (hereafter GC), also known as the Sea of Cortez, is located at the northwest of Mexico between the Baja California peninsula and Sonora and Sinaloa counties. The GC encompasses more than 800 islands. The average bathymetry in the GC depth varies from around 40 to 200 m in the upper gulf to 3,600 m at its entrance with the Pacific Ocean. It also contains several deep basins, such as Tiburon, Delfin and Wagner which are 400, 800 and 200 m deep, respectively. The northern Gulf of California as this is the area with the biggest potential for tidal-range energy exploitation given the tidal-range here is over 6 m [19].The Midriff region contains some important Islands, such as Smith, Salsipuedes, San Lorenzo, San Esteban Islands. The biggest of the Gulf islands are Angel de la Guarda and Tiburon. The areas of most interest to this study, is the region around the Midriff Islands in the central region, as a previous study indicates that currents in this region exceed 1.5 m/s [20] and hence there is potential for tidal-stream energy exploitation [16].

A depth-averaged barotropic model of the Gulf of California was previous configured by [16] using the TELEMAC modelling suite of tools [21]. Here we briefly describe the configuration and validation of that model and then we discuss the sensitivity tests we have undertaken. The TELEMAC modelling suite was chosen because of its: (1) computing performance - parallel processing, using the University of Southampton's supercomputer, IRIDIS, optimized simulation times; (2) finite element method, which enables variable mesh resolution to focus modelling effort in regions of interest; and (3) model inputs and outputs are compatible with a number of pre and post-processing software (e.g. Blue Kenue, Fudaa, MATISSE, Janet). TELEMAC is a popular model choice for tidal energy resource assessment and characterization (e.g., [22], [12] and [6]).

The model mesh is shown in Fig. 1a and c, and was configured using the Blue Kenue software. The model grid consists of 38,181 nodes and 133,779 elements. It has a resolution of 0.507◦ (~60 km) at the open boundary condition in the Pacific and increases to 0.042◦ (~5 km) at the entrance to the GC. Within the GC the resolution increases to 0.0083◦ (~1 km) around the energetic Midriff Islands and reduces to 0.025◦ (~3 km) resolution at the northern most reaches, where current speeds are low.

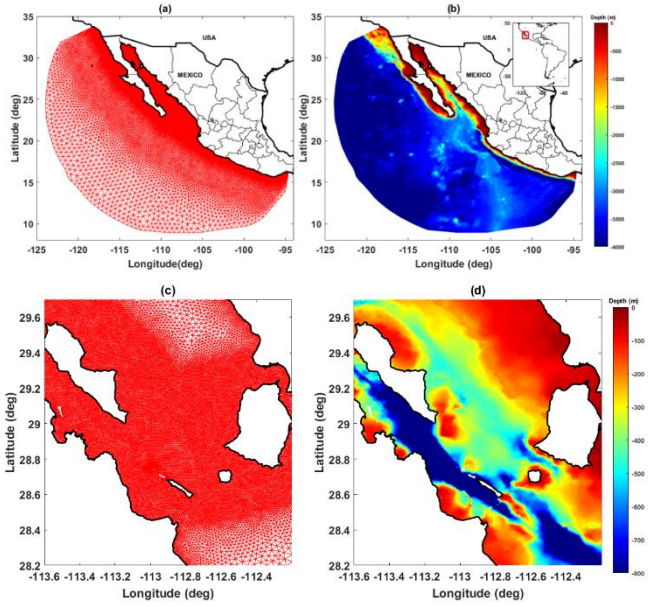

Fig. 1. Model gird for the (a) whole domain area and (c) just the Midriff area. Combined bathymetry used (GEBCO+CICESE) for (b) whole domain area and (d) just the Midriff area.

The model was extensively validated against tide gauge and ADCP (acoustic Doppler current profiler) measurements to ensure the accuracy of the predicted hydrodynamic conditions in the GC. Data for 11 tide gauge stations (see reference [16] for more details) located in the GC region and along the Mexican Pacific ocean coastline were obtained from CICESE, along with current velocity data from 4 ADCP stations. Sensitivity tests were undertaken using a range of uniform and spatially varying bottom friction coefficients. The Manning's law used and a final spatially uniform value of 0.030 s/m$^{1/3}$ was chosen as this resulted in the best validation.

Different methods were used to assess the performance of the hydrodynamic model in reproducing tidal levels and tidal currents at each observational site. To determine how accurately the model predicts both the tidal levels and currents in the region, the amplitude and phase of the eight main tidal constituents, extracted from both the measured and predicted water levels using the T_TIDE Matlab software package [23], were compared. In addition, three validation metrics were used to quantify the model skill. For each of the time-series, the absolute difference between each hourly measured and predicted value was computed. The mean, equivalent to the root mean square error (RMSE) and standard deviation of the absolute differences

were calculated. Correlation coefficients between the measured and predicted time-series were also derived for each complete time-series.

The spatial variations in tidal level constituents from the model predictions were compared to the OTIS tidal level constituents. The OTIS (OSU Tidal Inversion Software) model has been assimilated with Satellite Altimetry data and hence is considered as ground truth. The amplitudes and phases of the main semidiurnal (M_2, S_2) tidal constituents are shown in Fig. 2 and 3, respectively. Overall, the model is successful in reproducing the spatial distributions of both the amplitude and phase of the main tidal constituents. The model predictions capture the higher tidal amplitudes in the northern most reaches of the GC.

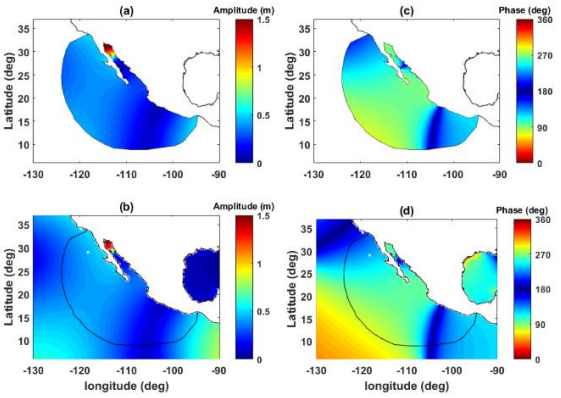

Fig. 2. M_2 amplitude predicted by (a) OTIS model (b) TELEMAC model, M_2 phase predicted by (c) OTIS model (d) TELEMAC model.

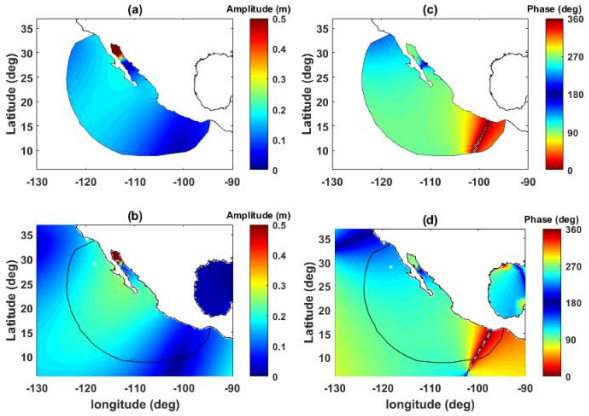

Fig. 3. S_2 amplitude predicted by (a) OTIS model (b) TELEMAC model, S_2 phase predicted by (c) OTIS model (d) TELEMAC model.

B. Sensitivity tests methods

Two main sensitivity tests were undertaken. First, we examined how current speeds, mean kinetic power density and annual mean power estimates, varied when using different bathymetric products. We ran two simulations, using just bathymetry data from two well-known and well-used sources: (1) GEBCO [17] and (2) ETOPO [18], which are available at resolutions of ~900 and ~775 m, respectively. A third run used the GEBCO data merged with the higher resolution data from the survey bathymetry data collected by CICESE (Fig. 4), for the Midriff region and the northern GC. The bathymetry data sets were combined using a merge function in ArcGIS software. Note, none of the points from either the GEBCO or CICESE data sets were omitted or altered. A cross-sectional from the central region of the GC is show in Fig. 5 highlighting the main differences for the three different products utilized in this work. The inclusion of the higher-resolution bathymetry data in the northern GC significantly improved the tidal level and current validation, compared to using just the GEBCO bathymetry alone.

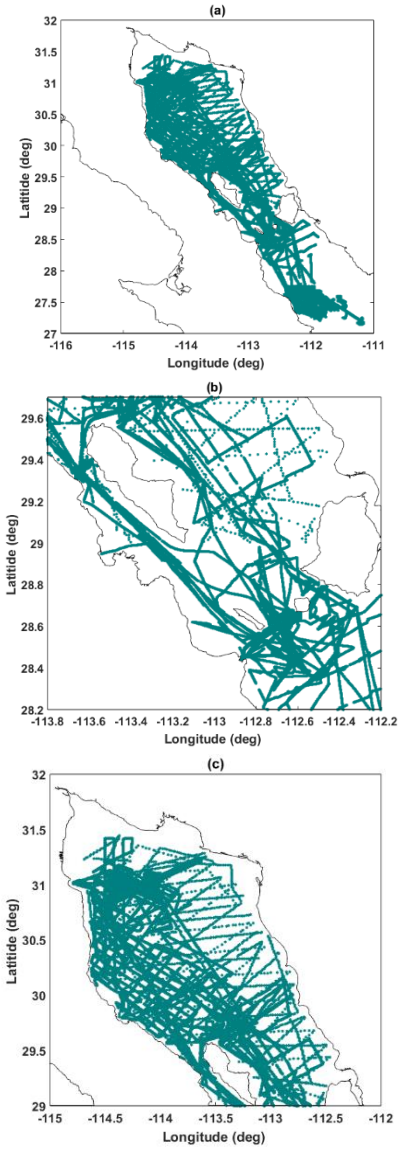

Fig. 4. Bathymetry survey by CICESE research centre for the: (a) Gulf of California; (b) midriff area; and (c) northern Gulf of California.

Second, we examined how current speeds, mean kinetic power density and annual mean power estimates, varied depending on which tidal constituents were used to force the model at the open boundary. The open ocean boundaries were driven using tidal levels predicted from the TPXO 7.2 dataset [24], [25]. We ran the model for a 1 month period and carried out a harmonic analysis on the predicted tidal levels, using the Matlab T_TIDE software [23]. First, we estimated the peak current speed, mean kinetic power density and annual mean power, considered all the 29 tidal constituents returned by the T_TIDE

harmonic analysis [16]. Then, the KPD and the annual maximum theoretical undisturbed mean power, was calculated considering: (1) only the M_2 tidal constituent; (2) only the S_2 constituent, and (3) the M_2 plus S_2 constituent.

III. RESULTS

C. *Bathymetry sensitivity*

Three percentage errors were calculated to quantify the model skill at the 4 ADCP locations. The largest error of the v component is at Ballenas channel using the GEBCO (16.97%) and ETOPO (26.12%) datasets on their own (Table I). This specific location has water depths between 800 and 900 m and therefore we assumed that these bathymetry products influence negatively with the v and u component. The smallest errors for u and v components are at Delfin basin with 2.7% and 3.7% when using the combined bathymetry GEBCO+CICESE. Therefore, we can conclude that the more precise bathymetry data can contribute significantly to the ADCP validation. Consequently, energy resource would be estimated more accurate.

TABLE I
PERCENTAGE ERROR OF U AND V VELOCITY COMPONENTS USING DIFFERENT BATHYMETRY PRODUCTS

Site Name	% Error GEBCO u	% Error GEBCO v	% Error ETOPO u	% Error ETOPO v	% Error GEBCO+ CICESE u	% Error GEBCO+ CICESE v
San Lorenzo	13.81	11.38	11.82	5.89	11.3	8.5
San Esteban	14.77	9.20	12.55	4.31	11.5	6.7
Ballenas Channel	3.25	16.97	15.28	26.12	6.7	25.0
Delfin	8.50	5.99	2.92	3.28	2.7	3.7
Mean	**10.08**	**10.88**	**27.1**	**9.90**	**8.04**	**11**

We compared the maximum current speeds and the estimated 'theoretical' power from these two runs, to the third run which used the GEBCO data merged with the higher resolution data from CICESE, for the Midriff region (Fig. 5c and Fig. 6c).

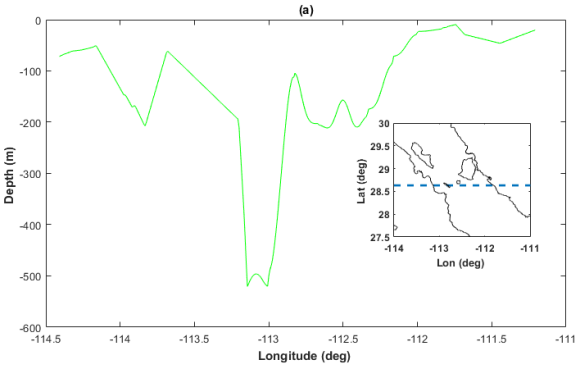

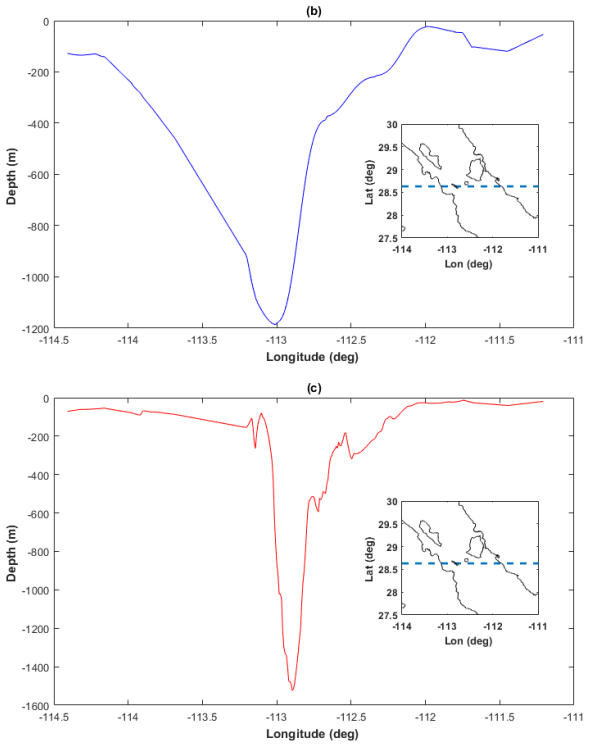

Fig. 5. Bathymetry cross-sectional profile (location showed in inlay in panel a) considering: (a) just GEBCO data, (b) just ETOPO data and (c) GEBCO plus CICESE merged data sets.

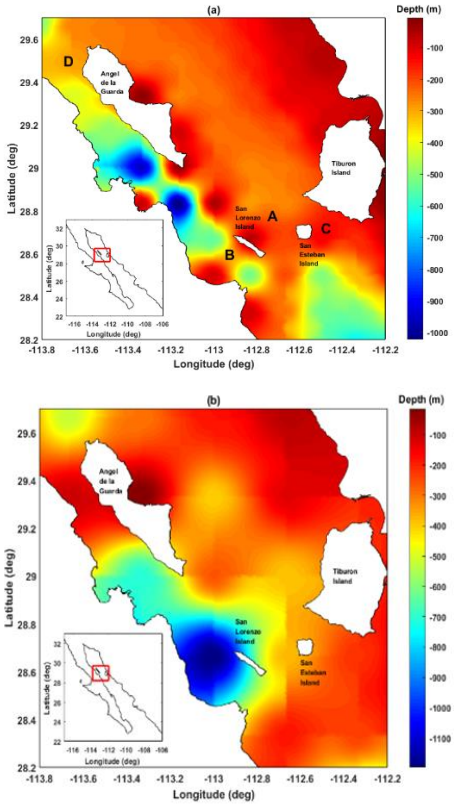

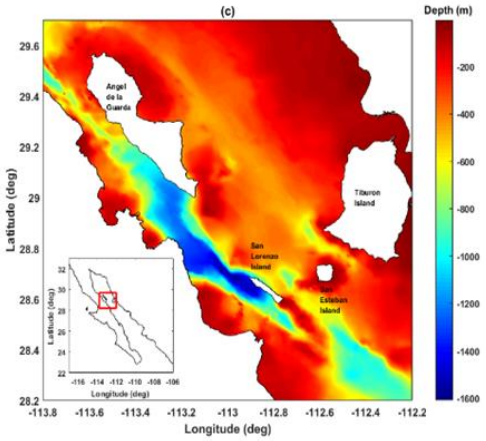

Fig. 6. Model bathymetry created using: (a) just GEBCO, (b) just ETOPO and (c) GEBCO and CICESE merged, for the Midriff area.

The current speed vary significantly across the three different bathymetry products within the four main regions where current speeds exceed 1 m/s (Fig. 7).

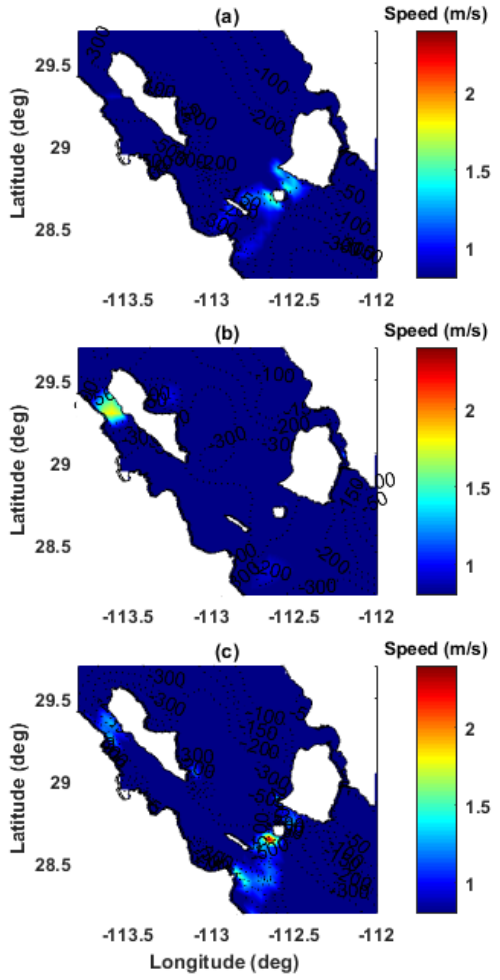

Fig. 7. Maximum current speed calculated using (a) GEBCO data only, (b) ETOPO data only and (c) GEBCO + CICESE merged bathymetry. Bathymetric contours are superimposed in m. All figures include the 29 tidal constituents originally used the model set up by [16].

The largest current speed were localised between San Lorenzo and San Esteban Island (herein San Lorenzo Passage) (Marker A on Fig. 6a) reaching a maximum of about 2.4 m/s in the deeper-water (~500 m) for the combined bathymetry data. In contrast, using GEBCO and ETOPO bathymetry products along, the current speeds reduce to around 1.2 m/s and 0.8 m/s respectively. Similarly in the region of Ballenas channel (Marker D on Fig. 6a) which is form between Angel de la Guarda Island and the Baja California Peninsula, relatively large differences were found. At the same location, the flow speed was estimated of around 1 m/s when using the combined bathymetry whereas using the GEBCO product, the current speed reduces to 0.5 m/s. However, the used of ETOPO bathymetry overestimated the current speed within Ballenas channel to around 1.8 m/s (Fig. 7b) as a comparison with the simulation which includes the combined bathymetry data GEBCO+CICESE where the current speed were found as 2.4 m/s.

The mean KPD and annual mean power are significantly underestimated when using just the GEBCO or ETOPO bathymetry data sources on their own in the Midriff region (Fig. 8).

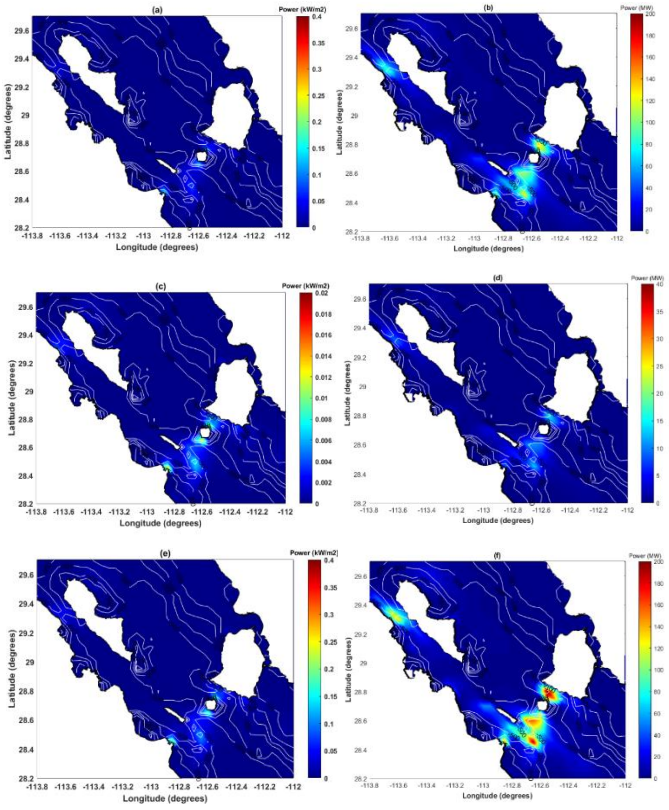

Fig. 8 (a,c,e) Annual mean kinetic power density, (c,f,i) Annual mean power and (b,d,f), (a,b) GEBCO only; (c,d) ETOPO only and (e,f) GEBCO data merged with the higher resolution data from CICESE, for the Midriff region. Bathymetric contours superimposed in m above.

For the region with fastest current speeds, San Lorenzo Passage (Marker A on Fig. 6a) the annual mean power is estimated to be 120 MW and 20 MW when using GEBCO and ETOPO runs, respectively (Fig. 8a and 8c); whereas the annual mean power was calculated as ~200 MW when using a bespoke dataset that was a combination of GEBCO and bathymetry provided by CICESE (Fig. 8f).

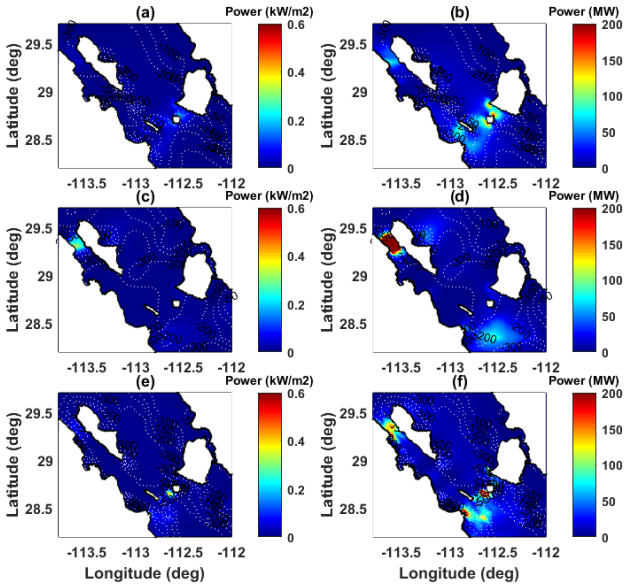

Fig. 9. Annual mean kinetic power density (a) just the M_2 constituent, (c) S_2 constituents (e) M_2 plus S_2 constituents. Annual theoretical mean power for (b) just the M_2 (d) S_2 constituents (f) M_2 plus S_2 constituents. All plots use the GEBCO data merged with the higher resolution data from CICESE, for the Midriff region, for the model bathymetry. Bathymetric contours superimposed in m above.

D. Tidal constituent sensitivity

The results of the tidal constituent sensitivity tests are shown in Fig. 9. The annual mean KPD, estimated using only the S_2 tidal constituent (Fig. 9c), decreased by around a third in the San Lorenzo Passage (Marker A on Fig. 6a) as compared with the calculation made using just the M_2 constituent (Fig. 9a), from around 0.18 to 0.08 kW/m^2 while the maximum value reached was ~0.25 kW/m^2 where the fasters currents occur. Consequently, there are significant differences for the estimation of annual maximum theoretical undisturbed mean power calculations when utilising M_2 and S_2 on their own in San Lorenzo Passage. Using just the M_2 tidal constituent, the estimation of the annual power is approximately between 90 and 100 MW (Fig. 9b). When using just the S_2 tidal constituents the annual power reduces by more than half to around 15 to 20 MW (Fig. 9d). Similarly, the annual mean power was calculated using the M_2 plus S_2 constituents and the results indicated an annual mean power range of 140 to 150 MW (Fig. 9f). Including all 29 tidal constituents, the maximum annual mean was estimated as ~200 MW. The mean annual power reduces significantly to around 70% using just M_2 plus S_2 tidal constituent from approximately 200 MW to between 140 to 150 MW.

IV. CONCLUSIONS

The aim of this paper has been to examine how choice of bathymetry product and tidal constituents affects the quantification of the tidal-stream energy resource for the GC. We compared three different bathymetry products and found that the tidal-stream energy resource was underestimated by as much as 75% when using just freely available global productions. We then compared the estimated energy using 29 tidal constituents with simulations that just included the M_2 and/or S_2 tidal constituents. The annual mean KPD reduced by almost 1/3rd in San Lorenzo Passage (Marker A on Fig. 6a), when just considering the M_2 and S_2 constituents, suggesting that diurnal and higher order harmonic constituents are important for accurate resource assessments in this region. Most previous tidal-stream assessments studies do not take into account the variability of the predicted tidal velocities as a result of the effect of the bathymetry data and consequently the mean annual power variations. Therefore, including higher resolution bathymetry data suggested that the tidal-stream resource of the Gulf of California to be higher than initial estimates with publicly available/low resolution coarse data products, which has interesting applications for the potential global resource and tidal energy industry size. In addition, we recommend to include the main semi-diurnals and diurnals constituents to assess more accurately the tidal-stream energy resource at any given site. Also importantly mention is that there was not any particular reason for not including a possible data combination of ETOPO+ CICESE. Then the best validation was obtained utilising GEBCO+CICESE data sets.

ACKNOWLEDGEMENT

We thank Dr. Silvio Guido Marinone and Dr. Antonio Gonzalez Fernandez from CICESE research centre for providing the higher resolution bathymetry data for the Gulf of California and Dr. Manuel Lopez from CICESE for the ADCP dataset.

REFERENCES

[1] Bahaj, A. & Myers, L., (2004). Analytical Estimates of Energy Yield Potential from the Alderney Race (Channel Islands) using Marine Current Energy Converters. Renewable Energy, 29, pp.1931-45.

[2] Bahaj, A. S. (2011). Generating electricity from the oceans. Renewable and Sustainable Energy Reviews, 15, 3399-3416.

[3] Lim, Y. S. & Koh, S. L. (2010). Analytical assessments on the potential of harnessing tidal currents for electricity generation in Malaysia. Renewable Energy, 35, 1024-1032.

[4] González-Gorbeña, E., Rosman, P. C. C. & Qassim, R. Y. (2015). Assessment of the tidal current energy resource in São Marcos Bay, Brazil. Journal of Ocean Engineering and Marine Energy, 1, 421-433.

[5] Lewis, M., Neill, S. P., Robins, P. E. & Hachemi, M. R. (2015). Resource assessment for future generations of tidal-stream energy arrays. Energy, 83, 403-415.

[6] Coles, D. S., Blunden, L. S. & Bahaj, A. S. (2017). Assessment of the energy extraction potential at tidal sites around the Channel Islands. Energy, 124, 171-186.

[7] Goward Brown, A. J., Neill, S. P. & Lewis, M. J. (2017). Tidal energy extraction in three-dimensional ocean models. Renewable Energy.

[8] Wang, T. & Yang, Z. (2017). A modeling study of tidal energy extraction and the associated impact on tidal circulation in a multi-inlet bay system of Puget Sound. Renewable Energy.

[9] Campbell, R., Martinex, A., Letetrel, C. & Rio, A. (2017). Methodology for estimating the French tidal current energy resource. International Journal of Marine Energy, 19, 256-271.

[10] Cornett A. (2006), Inventory of Canada's Marine renewable energy resources. Canadian Hydraulics centre. CHC-TR-041. April 2006.

[11] Tarbotton, M. & Larson, M. (2006). Canada ocean energy atlas (phase 1) potential tidal current energy resources analysis background. Report to Canadian Hydraulics Centre.
[12] Cornett A, Noemie Durand, Martin Serrer (2010). 3-D Modelling and Assessment of Tidal Current Resources in the Bay of Fundy, Canada 3rd International Conference on Ocean Energy, 6 October, Bilbao.
[13] Defne, Z., Haas, K. A. & Fritz, H. M. (2011). Numerical modelling of tidal currents and the effects of power extraction on estuarine hydrodynamics along the Georgia coast, USA. Renewable Energy, 36, 3461-3471.
[14] Adcock, T. A. A., Draper, S., Houlsby, G. T., Borthwick, A. G. L. & Serhadlıoğluet, S. (2013). The available power from tidal stream turbines in the Pentland Firth. Proceedings of the Royal Society A: Mathematical, Physical and Engineering Science, 469.
[15] Plew, D. R. and C. L. Stevens (2013). "Numerical modelling of the effect of turbines on currents in a tidal channel – Tory Channel, New Zealand." Renewable Energy 57: 269-282.
[16] Mejia-Olivares, C. J., Haigh, I. D., Wells, N. C., Coles, D. S., Lewis, M. J. & Neill, S. P. (2018). Tidal-stream energy resource characterization for the Gulf of California, México. Energy, 156, 481-491.
[17] Kapoor, D.C., (1981). General bathymetric chart of the oceans (GEBCO). Marine Geodesy, 5(1), pp.73–80.
[18] NOAA (2017). ETOPO1 Global Relief Model [online] United States of America. Available from https://www.ngdc.noaa.gov/mgg/global/. [Accessed March 2017].
[19] Mejia-Olivares, C.J., Haigh. I.D., Angeloudis A., Lewis, M. and Neill, S.P, 2019. The potential for tidal range energy resource in the Northern Gulf of California, México. In review.
[20] Badan-Dangon, A., M. C. Hendershott, and M. F. Lavın (1991), Underway Doppler current profiles in the Gulf of California, Eos Trans. AGU, 72(209), 217 – 218.
[21] Jean-Michel Hervouet, "Hydrodynamics of Free Surface Flows: Modelling with the Finite Element Method", Wiley Blackwell, April 2007, 360p, ISBN-13: 978-0470035580.
[22] Blunden, L. & Bahaj, A., (2006). Initial Evolution of Tidal Stream Energy Resources at Portland Bill, UK. Renewable Energy, 31, pp.121-32.
[23] Pawlowicz R, Beardsley B, Lentz S (2002). Classical tidal harmonic analysis including error estimates in MATLAB using T_TIDE. Comput Geosci. 28(8):929–37.
[24] Egbert, G. D., A. F. Bennet, and M. G. G. Foreman (1994), Topex/Poseidon tides estimated using a global inverse model, Journal of Geophysical Research, 99, 24,821 24,852.
[25] Egbert, G. D. and S. Y. Erofeeva (2002). "Efficient Inverse Modeling of Barotropic Ocean Tides." Journal of Atmospheric and Oceanic Technology 19(2): 183-204.